Chinese Chemical Letters 34 (2023) 107613

Contents lists available at ScienceDirect

Chinese Chemical Letters

journal homepage: www.elsevier.com/locate/cclet

Highly lipophilic coumarin fluorophore with excimer-monomer transition property for lipid droplet imaging

Xiang Shi[1], Ge Gao[1], Xiaoyang Liu, Lingling Xu, Yu Deng, Rui Wang*, Gaolin Liang*

State Key Laboratory of Bioelectronics, School of Biological Science and Medical Engineering, Southeast University, Nanjing 210096, China

ARTICLE INFO

Article history:
Received 4 March 2022
Revised 13 June 2022
Accepted 14 June 2022
Available online 18 June 2022

Keywords:
Excimer-monomer transition
Fluorescent probe
Hydrophobicity
Lipid droplets
Monomer emission

ABSTRACT

Lipid droplet (LD) fluorescent imaging plays an important role in the detection of lipid-related diseases. Due to their poor photostability and low hydrophobicity of currently available LD imaging fluorophores, LD imaging is limited by its short imaging period and low imaging contrast. Herein, we reasonably designed a highly lipophilic compound Cou-Flu with excellent photostability and excimer-monomer transition property. It exhibited weak excimer emission in cytoplasm, but strong monomer emission in LDs, enabling high contrast LD imaging and LD movement tracing in cells. Zebrafish imaging study demonstrated that Cou-Flu was also suitable for *in vivo* LD detection with excellent sensitivity. We anticipate that Cou-Flu could be widely applied to understand LD-related intracellular activities and even LD-related diseases in the future.

Lipid droplets (LDs) are dynamic complex organelles and a typical LD is composed of a phospholipid monolayer and a neutral lipid core [1,2]. Known as lipid reservoirs to provide essential energy for normal physiological functions in cells [3,4], LDs are also closely associated with many lipid-related diseases. For example, an increasing number of LDs has been found in obesity, fatty liver, diabetes, and various cancers (*e.g.,* colon, cervical, liver, and brain cancers) [5–8]. Thus, the development of an effective tool to monitor LDs in living organisms (such as cells and animal models) in real-time holds great promise for scientific bio-research and health care.

Due to its high sensitivity and spatiotemporal resolution, fluorescence imaging has become a promising tool for visualizing cellular dynamics [9]. Up to date, many fluorescent probes have been commercialized for LD staining, such as Nile Red, BODIPY 493/503, LipidTox Red, Oil red O. Among these probes, lipidTOX Red and Oil red O are limited for fixed cells only. In comparison, Nile Red and BODIPY 493/503 are more suitable for imaging LDs in living cells and animal models due to their low toxicity [10,11]. Nevertheless, these two probes still have some intrinsic drawbacks. For example, Nile Red suffers from low molecular lipophilicity. As a result, besides LDs, it also stains other organelles (particularly ER, Golgi, mitochondria, *etc.*) in real practice [12,13], yielding a high background fluorescence and low signal-to-noise ratio of LDs in living cell imaging [14]. Despite it having a more hydrophobic conjugated aromatic structure (dipyrromethene-boron difluoride) [15–17], which provides stronger affinity to LDs, the "Achilles' heel" of BODIPY 493/503 is its small Stokes shift (~10 nm) and photobleaching effect [18–20]. Small Stokes shift will cause severe self-absorption phenomenon and thus weaken the fluorescence. Meanwhile, its low photostability may hinder the continuous monitoring of the dynamic processes of LDs in real time. Nevertheless, in the last decade, much effort has been devoted to develop more efficient LD probes, such as metal complexes [21,22] and AIE-active compounds [23–25]. In 2015, Ir(III) complexes were reported to label LDs with great photostability and large Stokes shift. But their relatively low hydrophobicity and values of lop (octanol-water partition coefficient, 1.7-2.1) lead to low selectivity to LDs [21]. In order to improve the selectivity, a series of AIEgens were designed and applied for LD imaging. Although these AIE fluorophores have great hydrophobicity and excellent selectivity, their LD imaging sensitivity is still too low due to the aggregation-enhanced emission (AEE) effect, which increases the background signal of cytoplasm [11]. Therefore, it is highly desired to develop an imaging probe with both high LD selectivity and high sensitivity for LD imaging.

Thus, we proposed to design a new fluorophore with high photostability for monitoring LD dynamics in living organisms. To our knowledge, 7-(diethylamino)coumarin-3-carboxylic acid (Cou) has been widely used as a fluorescent bioimaging probe due to its high photostability and fluorescence quantum yield, as well as

* Corresponding authors.
E-mail addresses: ruiwang938@seu.edu.cn (R. Wang), gliang@seu.edu.cn (G. Liang).
[1] These authors contributed equally to this work.

https://doi.org/10.1016/j.cclet.2022.06.036
1001-8417/

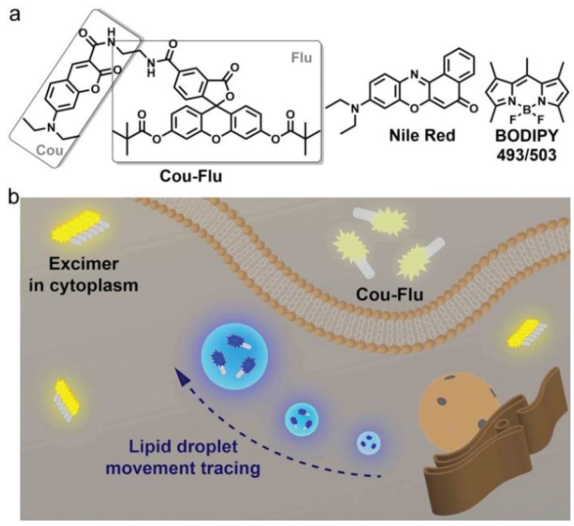

Fig. 1. (a) Structures of Cou-Flu, Nile Red and BODIPY 493/503. (b) Schematic illustration for the excimer-monomer transition of Cou-Flu. In the cytoplasm, Cou-Flu mainly exists in the form of excimer and emits weak yellow emission. The blue-shifted photoluminescence along with ~20 times enhancement could be observed after it was accumulated in LDs as monomer.

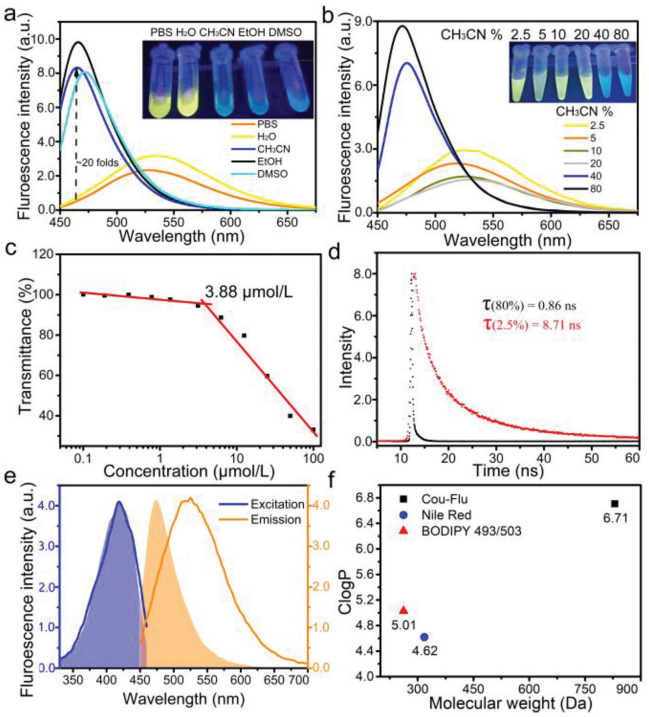

Fig. 2. Fluorescence spectra of Cou-Flu (a) in different solvents, and (b) in 2.5%–80% CH_3CN-water mixtures (λ_{ex} = 430 nm). Inset: photos of the corresponding solution under 365 nm irradiation by a handheld fluorescent lamp. Concentration: 25 mmol/L. (c) Critical aggregation concentration (CAC) of Cou-Flu in 2.5% CH_3CN fraction aqueous solution. (d) Time-resolved fluorescence decay of Cou-Flu in 80% CH_3CN fraction aqueous solution (λ_{ex} = 405 nm, λ_{em} = 480 nm) and 2.5% CH_3CN fraction aqueous solution (λ_{ex} = 405 nm, λ_{em} = 530 nm). (e) The excitation and emission spectra of Cou-Flu monomer (80% CH_3CN, shadows) and H-aggregates (2.5% CH_3CN, solid lines). (f) Clog*P* values of Cou-Flu, Nile Red, and BODIPY 493/503.

facile chemical modification ability [26–28]. However, the relatively low hydrophobicity of Cou makes it unsuitable to locate LDs with high selectivity. Therefore, we hypothesized that introduction of a highly lipophilic group to Cou might significantly increase its selectivity to LDs. According to the reported studies [29,30], 6-carboxyfluorescein derivatives unit (Flu) is a further extended aromatic system with excellent lipophilicity. Therefore, we are encouraged to couple Flu with Cou to construct a highly lipophilic coumarin fluorophore Cou-Flu (Fig. 1a). As expected, the LD selectivity of Cou-Flu has been significantly improved by comparing with Nile Red in cellular imaging. Meanwhile, we found that Cou-Flu only provides weak yellow fluorescence in water but exhibits a significant blue-shift (~50 nm) along with ~20 folds intensity enhancement after being transferred to organic solvents. Its fluorescence enhancement is much higher than that of the BODIPY 493/503 (~7 folds) at similar condition [31]. We verified that this phenomenon can be attributed to the polarity-induced excimer-monomer transition, as a result of the formation of H-aggregate. In contrast with the reported AIEgen, the H-aggregate of Cou-Flu does not exhibit the AEE effect, making it more sensitive in living organism imaging by reducing the background signal in the cytoplasm. Besides that, Cou-Flu also showed higher photostability than BODIPY 493/503, which can be explained by the accumulation of Cou-Flu hinders its destruction by free radicals of oxygen. As shown in Fig. 1b, Cou-Flu could effectively image LDs in common living cells, while it mainly maintained the excimer form in the cytoplasm with a weak signal. Upon accumulation in the LDs, the fluorescence intensity of Cou-Flu increased significantly, which is attributed to its excimer-monomer transition. Moreover, endogenous LDs in zebrafish can also be detected by Cou-Flu with excellent sensitivity.

We synthesized probe Cou-Flu with four steps and an overall yield of 69%, as shown in Scheme S1 (Supporting information). Compound **3** was obtained from commercially available 6-carboxyfluorescein (**2**) according to the reported method [32]. We initially treated compound **4** with *N*-Boc-ethylenediamine to afford compound **5** in great yield (98%). After that, **5** underwent a deprotection reaction with trifluoroacetic acid (TFA) to yield compound **6**, which condensed with **3** at room temperature to afford probe Cou-Flu in middle yield (78%). All the structures of compounds were characterized with electrospray ionization-mass spectrometry (ESI-MS), ^{1}H NMR and ^{13}C NMR (Figs. S1–S6 in Supporting information).

Subsequently, the absorption spectra of Cou-Flu were measured in solvents with various polarities, including water (H_2O), phosphate buffer saline (PBS), acetonitrile (CH_3CN), ethanol (EtOH), and dimethyl sulfoxide (DMSO). As shown in Fig. S7a (Supporting information), the centers of the main absorption peaks (~430 nm) of Cou-Flu were very close in different solvents, but relatively lower intensities were observed in the polar environment (H_2O and PBS), which might be attributed to the aggregation of Cou-Flu in aqueous solutions. We also found the fluorescence emission wavelength is solvent polarity-dependent (Fig. 2a). In detail, in aqueous solutions, weak broad signals centered at 530 nm were observed. While in organic solvents, the peak was shifted to 480 nm along with a 20-fold increase of fluorescence intensity. The fluorescence analysis on the Cou and Flu independently show that Cou is the main fluorophore with excellent dispersity in both polar and non-polar solutions (Figs. S7b and c in Supporting information), while Flu is non-fluorescent at the same condition and shows a higher Clog*P* value (5.08) than common self-assembling ligands, such as Py-OH (3.46), Py-COOH (3.61) and PBI (4.26) (Figs. S7d–g in Supporting information). As a result, the fluorescence 'turn-on' phenomenon of Cou-Flu should be associated with the molecular aggregation of its Flu fragment.

Given the fact that no unit in Cou-Flu was related to fluorescence change mechanisms of internal charge transfer (ICT), aggregation induced emission (AIE), Förster resonance energy transfer (FRET), or excited-state intramolecular proton transfer (ESIPT), we reasonably presumed that this phenomenon might be induced by

either excimer-monomer transition or chemical factors (structure-change). To determine the main affecting source, all the samples were characterized with ESI-MS. As shown in Fig. S8 (Supporting information), Cou-Flu exhibited excellent stability in different solvents. Therefore, it is reasonable to speculate that the observed blue-shift of the emission peaks and the significant increase of the fluorescence intensity of Cou-Flu are associated with its excimer–monomer transition, rather than chemical factors. To further investigate the transition between monomer and excimer in varied polarity, the spectra of Cou-Flu were measured in water containing various amounts of CH_3CN. As shown in Fig. 2b, Cou-Flu exhibited a weak emission maximum at 530 nm in the relatively polar environment (v_{CH_3CN}/v_{H_2O} less than 40%). After increasing the CH_3CN fraction to 40%, the peak positions shifted significantly from 530 to 480 nm. At the same time, the fluorescence color of Cou-Flu was changed from yellow to blue (inset, Fig. 2b), which suggested that a saturation point was reached where excimers transformed to the monomeric counterparts.

Next, the critical micelle concentration (CAC) of Cou-Flu in CH_3CN aqueous solution (2.5%, v/v) was measured to track the formation process of excimer. As shown in Fig. 2c, the formation of Cou-Flu aggregates could be observed at concentrations higher than 3.88 μmol/L, which was also confirmed by its transmission electron microscopy (TEM) image at 5 μmol/L (Fig. S9a in Supporting information). Additionally, the intramolecular motion would be restricted in the aggregate state of excimer, which inhibits the non-radiative decay, thereby facilitating the radiative release of the photo-excited energy [33]. As a result, a longer fluorescence lifetime of fluorescence dyes should be observed in excimer forms than in their monomeric counterparts [34,35]. Fig. 2d shows the fluorescence decays of Cou-Flu excited at 405 nm in CH_3CN aqueous solution with a volumetric fraction of 2.5% or 80%, respectively. The average fluorescence lifetime of the 530 nm peak was 10 times longer than that of the 480 nm peak, which further confirmed the formation of excimer. Meanwhile, to further investigate their specific aggregate types (H- or J-aggregates), the maximum excitation and emission of Cou-Flu (25 μmol/L) in above CH_3CN aqueous solutions were obtained. As shown in Fig. 2e, the excitation peaks of both emissions were located at 430 nm, matching the center of the main absorption peak (Fig. S9b in Supporting information), indicating that the two emissions (480 and 530 nm) were stemmed from the same ground-state absorption [36]. Moreover, the excimer emission (2.5% CH_3CN fraction solution) exhibited a significant red-shift (~50 nm) compared to monomer emission (80% CH_3CN fraction solution), implying that the main form of the excimers in our research was H-aggregates [37–39].

Additionally, detection selectivity of Cou-Flu towards LDs was also predicted through computational modeling. It is well known that LDs feature an inherent lipophilic core, thus excellent hydrophobicity and high log*P* value (>5) are necessary for organic dyes to specifically locate in LDs [40,41]. Herein, we estimated the value of Clog*P* (calculated log*P*) *via* ChemDraw Ultra 12.0 software. As shown in Fig. 2f, Cou-Flu exhibited a higher value of Clog*P* (6.71) than the commercial Nile Red (4.62) and BODIPY 493/503 (5.01), indicating that Cou-Flu may have a stronger affinity towards LDs. Furthermore, the effect of pH on Cou-Flu fluorescence properties was examined as well. No significant changes in the fluorescence spectra were observed when Cou-Flu was incubated in PBS solutions at pH values ranging from 4.5 to 8.5 (Fig. S10 in Supporting information), demonstrating the feasibility of Cou-Flu for LD imaging in the physiological environment (pH 5.5–8.0). Subsequently, we further compared the cytotoxicity of Cou-Flu with Nile Red. The results in Fig. S11 (Supporting information) showed that no distinct inhibition effect was observed in HepG2 cell growth when the cells were incubated with Cou-Flu, even at a Cou-Flu concentration up to 100 μmol/L. In contrast, the Nile Red started

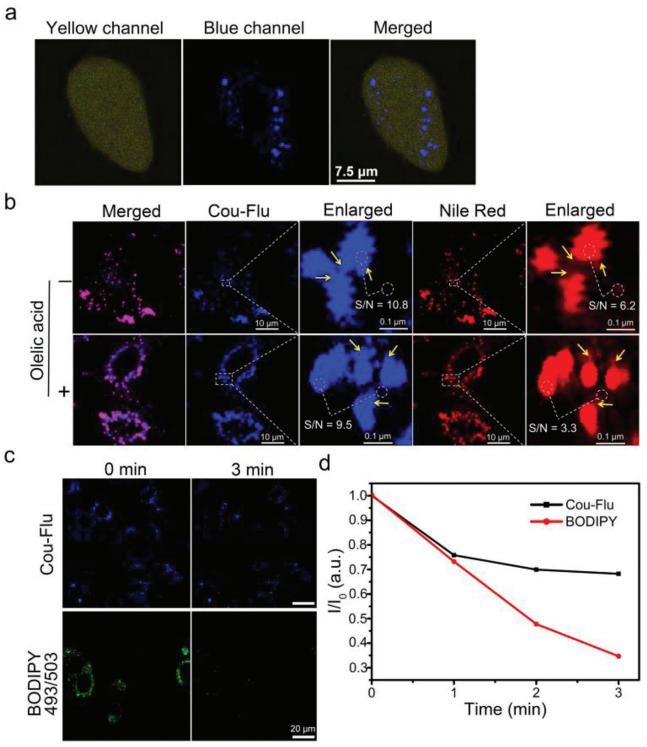

Fig. 3. (a) Confocal fluorescence images of HepG2 cells stained with Cou-Flu (12 μmol/L, λ_{ex} = 405 nm) for 20 min. Scale bar: 7.5 μm. (b) Confocal fluorescence images of Cou-Flu probe (10 μmol/L, blue, λ_{ex} = 405 nm) and Nile Red (12 μmol/L, red, λ_{ex} = 532 nm) co-stained HepG2 cells (with or without oleic acid treatment), respectively. Scale bars: 10 and 0.1 μm. The yellow arrow indicates the LDs that can be resolved by Cou-Flu but not by Nile Red. (c) The confocal fluorescence images of HeLa cells stained with Cou-Flu (λ_{ex} = 405 nm, 10 μmol/L, blue) and BODIPY 493/503 (λ_{ex} = 488 nm, 10 μmol/L, green) respectively at different irradiation time (0 or 3 min). Scale bar: 20 μm. (d) Time-dependent FL emission intensity of the cells in c. *I* represents cell FL intensity at a certain time point, while I_0 represents cell FL intensity at 0 min.

to exhibit obvious cytotoxicity at a concentration of 5 μmol/L. Moreover, to demonstrate the stability of Cou-Flu in cells, we co-incubated HepG2 cell lysates with the probe for 4 h. HPLC analysis of the incubation solution showed that, even in the presence of the carboxylesterase in cells, chemical structure of Cou-Flu was inact (Fig. S12 in Supporting information). These results indicated that Cou-Flu possesses excellent biocompatibility and chemical stability, enabling it suitable for LD imaging both *in vitro* and *in vivo.*

Subsequently, we chose HepG2 cells as the model cell lines to evaluate living cell imaging performance of Cou-Flu. After the cells were pretreated with oleic acid (a promoter for LD production in the cytoplasm) for 6 h, Cou-Flu was added and confocal fluorescence images of the cells at different time points (1, 3, 5, 10, 20 min) were recorded. As shown in Fig. 3a and Fig. S13 (Supporting information), weak yellow fluorescence signals (excimer emission) and bright blue fluorescence signals (monomer emission) could be observed in cytoplasm and LDs, respectively. These results demonstrated that Cou-Flu has a great permeation ability through the plasma membrane, thus successfully imaging LDs in cells. To further confirm whether Cou-Flu could selectively label LDs, Nile Red was used as a reference dye to perform the co-staining experiments. As shown in Fig. 3b, whether in the presence or in the absence of oleic acid, both Cou-Flu and Nile red could specifically target and light up the LDs in HepG2 cells, and an overlap ratio of more than 90% was obtained between them (Fig. S14 in Supporting information), suggesting that Cou-Flu could be applied as an effective tool for LD imaging. Moreover, the zoomed-in images

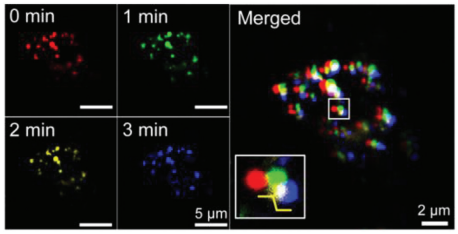

Fig. 4. Confocal fluorescence images recorded at different time points for tracking the dynamic positions of LDs in HepG2 cells by Cou-Flu probe (12 μmol/L, λ_{ex} = 405 nm). Four pseudo-colors indicate the moving trajectory of LDs at different time points (0–3 min). Scale bars: 5 μm and 2 μm, respectively.

reveal that Cou-Flu provided more structural details than Nile Red on the same LDs (Fig. 3b). In detail, Cou-Flu showed 1.7 times (10.8 *vs.* 6.2) and 2.9 times (9.5 *vs.* 3.3) higher signal to noise (S/N) ratios than those of Nile Red without or with oleic acid, respectively (Fig. 3b). These results suggest that our Cou-Flu probe has higher detection sensitivity and wider dynamic range (*i.e.*, detectable lipid concentration) than the commercial Nile Red dye for LD imaging. To further expand the application of Cou-Flu for imaging LDs in different cell lines, we chose MDA-MB-231, 4T1, MCF-7, MCF-10A, HeLa and L02 cells as models to perform co-staining experiments. As displayed in Fig. S15 (Supporting information), the high coefficient values range from 0.87 to 0.92 revealed that Cou-Flu could be widely used for imaging LDs in different cell lines.

Besides imaging sensitivity, photostability is another concern in the real-time tracking of LDs dynamics. As is known to all, prolonged excitation time generally leads to a significant decrease in the fluorescence intensity of many fluorescent probes. To investigate the photostability of Cou-Flu, commercial LD probe BODIPY 493/503 was employed as a reference. As shown in Figs. 3c and d and Fig. S16 (Supporting information), the fluorescence intensity loss of Cou-Flu was negligible compared with that of BODIPY 493/503 under successive irradiation at the same power density for 3 min. These results indicate that Cou-Flu has much better photostability than BODIPY 493/503, making it more favorable for real-time LD tracking.

Owning to its excellent LD selectivity, biocompatibility, and photostability, we attempted to further explore the capability of Cou-Flu in imaging cellular LD dynamics. It is well known that the dynamic movements of LDs in living cells are closely related to the LD metabolism and intracellular organelle interaction [27]. Therefore, monitoring the changes of LD position in a real-time manner is of great importance in physiology and pathology. Cou-Flu was incubated with HepG2 cells, and then the cells were imaged under a confocal microscope at different time points (0–3 min). As shown in Fig. 4, Cou-Flu displayed excellent LD dynamic tracking performance. In addition, known as the energy-storing organelles in cells, LDs also play an important role in coping with cellular energy shortage. When cells are under starvation conditions, LDs can provide cells with the necessary energy to survive through lysosome-mediated autophagy, known as lipophagy [42]. As a proof of concept, we tried to track the process of lipophagy according to the reported method [43]. Cou-Flu and LysoTracker Red were co-incubated with HepG2 cell lines, and fluorescence imaging was performed as the cells were under starvation conditions in different stages. The results in Fig. S17 (Supporting information) demonstrated that no distinct interactions between LDs and lysosomes were observed when the cells were under starvation treatment for 15 min. With prolonged starvation time (6 or 12 h), a significant overlap of red (LysoTracker Red emission) and blue (Cou-Flu emission) fluorescence could be observed, indicating that the process of lipophagy occurred in the cells (Fig. S17).

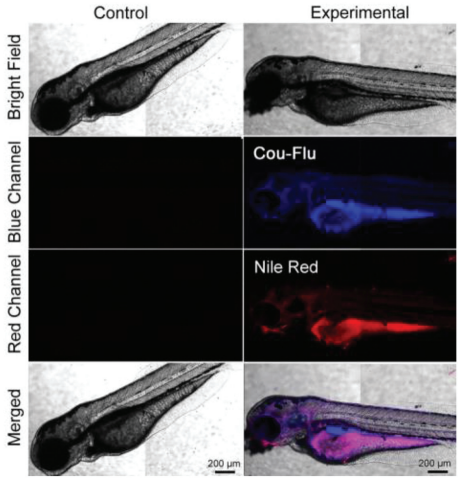

Fig. 5. Co-localization imaging of untreated zebrafish (left), and zebrafish stained with Cou-Flu and Nile Red (right). λ_{ex} = 405 nm for Cou-Flu; λ_{ex} = 532 nm for Nile Red. Scale bar: 200 μm.

Based on above results, it is confirmed that Cou-Flu is a promising organic probe that could be used not only for real-time LD monitoring in living cells, but also for observing the physiological processes of LDs.

Finally, we investigated the *in vivo* LD imaging capability of Cou-Flu on a 4-day-old zebrafish. As displayed in Fig. 5, the control zebrafish, which has no treatment, exhibited almost no fluorescence in both channels (405 and 532 nm) under the laser confocal microscope. In comparison, when the zebrafish were co-incubated with Cou-Flu and Nile Red for 24 h at room temperature, bright blue (Cou-Flu fluorescence emission) and red (Nile Red fluorescence emission) signals could be observed in the corresponding channel respectively. Furthermore, the high coincidence degree between the two channels further confirmed our probe Cou-Flu has a great potential for tracing LDs in zebrafish.

In summary, we reasonably designed a highly lipophilic coumarin fluorophore Cou-Flu with excimer-monomer transition property, which enables it real-time monitoring of LDs both *in vitro* and *in vivo*. It exhibited weak excimer emission in the cytoplasm, but much stronger monomer emission turning on in LDs. *In vitro* studies demonstrated that polarity-dependent excimer–monomer transition of Cou-Flu is the key mechanism behind this phenomenon. Moreover, compared to conventional fluorophores, Cou-Flu can stain LDs in living cells with higher selectivity, imaging S/N, and photostability. These features make it beneficial in real-time LD monitoring and observing the physiological processes of LDs in living cells. Significantly, *in vivo* experiments demonstrated that Cou-Flu has a great potential in visualizing LD metabolism within living subjects. We foresee that our probe Cou-Flu could serve as a promising tool to understand LD-related intracellular activities, as well as for studying LD-related diseases in the near future.

Declaration of competing interest

The authors declare that they have no known competing financial interests or personal relationships that could have appeared to influence the work reported in this paper.

Acknowledgment

This work was supported by the National Natural Science Foundation of China (Nos. 21725505, 22074016 and 81821001).

Supplementary materials

Supplementary material associated with this article can be found, in the online version, at doi:10.1016/j.cclet.2022.06.036.

References

[1] R.V. Farese, T.C. Walther, Cell 139 (2009) 855–860.
[2] J. Zheng, S. Qin, L. Gui, et al., Chin. Chem. Lett. 32 (2021) 2385–2389.
[3] Y.H. Pan, X.X. Chen, L. Dong, et al., Chin. Chem. Lett. 32 (2021) 3895–3898.
[4] Z. Sun, Y. Liu, P. Guan, et al., Dyes Pigment. 185 (2021) 108884.
[5] J.C. Cohen, J.D. Horton, H.H. Hobbs, Science 332 (2011) 1519–1523.
[6] A.M. Dvorak, P.F. Weller, V.S. Harvey, et al., Int. Arch. Allergy Immunol. 101 (1993) 136–142.
[7] A.S. Greenberg, R.A. Coleman, F.B. Kraemer, et al., J. Clin. Invest. 121 (2011) 2102–2110.
[8] N. Krahmer, R.V. Farese, T.C. Walther, EMBO Mol. Med. 5 (2013) 973–983.
[9] M. Vendrell, D. Zhai, J.C. Er, et al., Chem. Rev. 112 (2012) 4391–4420.
[10] T.K. Fam, A.S. Klymchenko, M. Collot, Materials 11 (2018) 1769–1788.
[11] P. Greenspan, E.P. Mayer, S.D. Fowler, J. Cell Biol. 100 (1985) 965–973.
[12] M. Collot, T.K. Fam, P. Ashokkumar, et al., J. Am. Chem. Soc. 140 (2018) 5401–5411.
[13] T. Felbeck, T. Behnke, K. Hoffmann, et al., Langmuir 29 (2013) 11489–11497.
[14] J. Chen, C. Wang, W. Liu, et al., Angew. Chem. Int. Ed. 133 (2021) 25308–25317.
[15] P.M. Gocze, D.A. Freeman, Cytometry 17 (1994) 151–158.
[16] A. Loudet, K. Burgess, Chem. Rev. 107 (2007) 4891–4932.
[17] A.H.M.M. Reza, Y. Zhou, J. Tavakoli, et al., Mater. Chem. Front. 5 (2021) 268–283.
[18] S. Karmann, S. Follonier, M. Bassas-Galia, et al., J. Microbiol. Methods 131 (2016) 166–171.
[19] D. Wang, H. Su, R.T.K. Kwok, et al., Adv. Funct. Mater. 27 (2017) 1704039.
[20] T. Yoshihara, R. Maruyama, S. Shiozaki, et al., Anal. Chem. 92 (2020) 4996–5003.
[21] L. He, J.J. Cao, D.Y. Zhang, et al., Sens. Actuators B: Chem. 262 (2018) 313–325.
[22] J. Tang, Y. Zhang, H.Y. Yin, et al., Chem. Asian J. 12 (2017) 2533–2538.
[23] M. Jiang, X. Gu, J.W. Lam, et al., Chem. Sci. 8 (2017) 5440–5446.
[24] C. Xu, H. Zou, Z. Zhao, et al., Adv. Funct. Mater. 29 (2019) 1903278.
[25] Z. Zheng, T. Zhang, H. Liu, et al., ACS Nano 12 (2018) 8145–8159.
[26] Y. Zhao, Q. Zheng, K. Dakin, et al., J. Am. Chem. Soc. 126 (2004) 4653–4663.
[27] H. Xu, H. Zhang, G. Liu, et al., Anal. Chem. 91 (2019) 977–982.
[28] Y. Zhong, J. Zhan, G. Xu, et al., Angew. Chem. Int. Ed. 60 (2021) 8121–8129.
[29] N. Zhou, F. Huo, Y. Yue, et al., Chin. Chem. Lett. 31 (2020) 2970–2974.
[30] Y. Wu, S. Huang, F. Zeng, et al., Chem. Commun. 51 (2015) 12791–12794.
[31] S. Choi, J. Bouffard, Y. Kim, Chem. Sci. 5 (2014) 751–755.
[32] T. Hirano, K. Kikuchi, Y. Urano, et al., J. Am. Chem. Soc. 122 (2000) 12399–12400.
[33] M. Gao, H. Su, S. Li, et al., Chem. Commun. 53 (2017) 921–924.
[34] G. Han, D. Kim, Y. Park, et al., Angew. Chem. Int. Ed. 54 (2015) 3912–3916.
[35] D. Chaudhuri, D. Li, Y. Che, et al., Nano Lett. 11 (2011) 488–492.
[36] T. Förster, Angew. Chem. 81 (1969) 1039–1045.
[37] J.D. Zhou, W.Q. Zhang, L.L. Liu, et al., Chin. Chem. Lett. 27 (2016) 1350–1356.
[38] I.A. Karpenko, M. Collot, L. Richert, et al., J. Am. Chem. Soc. 137 (2015) 405–412.
[39] F. Wuerthner, T.E. Kaiser, C.R. Saha-Moeller, Angew. Chem. Int. Ed. 50 (2011) 3376–3410.
[40] E.R. Sodre, B.C. Guido, P.E.N. de Souza, et al., J. Org. Chem. 85 (2020) 12614–12634.
[41] W. Yin, Y. Li, N. Li, et al., Adv. Opt. Mater. 8 (2020) 1902027.
[42] X. Zhang, L. Yuan, J. Jiang, et al., Anal. Chem. 92 (2020) 3613–3619.
[43] S. Adhikari, J. Moscatelli, E.M. Smith, et al., Nat. Commun. 10 (2019) 3400.